J|A|C|S
ARTICLES
Published on Web 02/06/2004

Measurements of Side-Chain $^{13}C-^{13}C$ Residual Dipolar Couplings in Uniformly Deuterated Proteins

Beat Vögeli,[†] Helena Kovacs,[‡] and Konstantin Pervushin*,[†]

Contribution from the Laboratorium für Physikalische Chemie, Swiss Federal Institute of Technology, ETH-Hönggerberg, CH-8093 Zürich, Switzerland, and Bruker AG, Industriestrasse 26, CH-8117 Fällanden, Switzerland

Received August 28, 2003; E-mail: kope@phys.chem.ethz.ch

Abstract: ^{13}C-only spectroscopy was used to measure multiple residual $^{13}C-^{13}C$ dipolar couplings (RDCs) in uniformly deuterated and ^{13}C-labeled proteins. We demonstrate that ^{13}C-start and ^{13}C-observe spectra can be routinely used to measure an extensive set of the side-chain residual $^{13}C-^{13}C$ dipolar couplings upon partial alignment of human ubiquitin in the presence of bacteriophages Pf1. We establish that, among different broadband polarization transfer schemes, the FLOPSY family can be used to exchange magnetization between a *J* coupled network of spins while largely decoupling dipolar interactions between these spins. An excellent correlation between measured RDCs and the 3D structure of the protein was observed, indicating a potential use of the $^{13}C-^{13}C$ RDCs in the structure determination of perdeuterated proteins.

Introduction

Uniform deuteration is frequently considered as a prerequisite for solution NMR structural studies of proteins with molecular weight larger than 30 kDa.[1−6] The use of deuteration in combination with transverse relaxation optimized spectroscopy (TROSY) enabled backbone resonance assignment in large soluble protein complexes[7−9] and integral membrane proteins solubilized in micelles.[10−14] Recently, uniform deuteration was proposed as a means to observe multiple long-range $^{1}H-^{1}H$ residual dipolar couplings (RDCs) even in small and medium-sized proteins.[15,16] Because protons are typically considered as the only structural probes located on the side chains, the depletion or complete replacement of side-chain protons with deuterons is frequently seen as an informational void in structural studies of large proteins.[12] Structural information for side chains not stemming from protons is available in the form of $^{13}C^{\alpha}-^{13}C^{\beta}$ RDCs.[17,18] Overall, the side-chain RDCs may prove indispensable for high-quality structure determinations of deuterated proteins. In addition, side-chain RDCs can potentially be employed to study side-chain dynamics.[19,20]

The 2D ^{13}C-observe technology for isotopically enriched proteins was introduced by the Markley group.[21,22] On the basis of this, we proposed a new strategy for side-chain assignment in large uniformly deuterated proteins.[23] The key element in this approach is the nearly complete assignment of the side-chain ^{13}C resonances achieved using ^{13}C-start and ^{13}C-observe experiments in combination with the broadband homonuclear cross polarization. A notable feature of the ^{13}C-observe experiments is that multiple and redundant $^{1}J_{CC}$ scalar couplings are resolved as ^{13}C multiplets in the directly acquired ^{13}C dimension. In the current paper, we provide a theoretical and practical basis for measurements of homonuclear $^{13}C-^{13}C$ RDCs stemming from deuterated side chains. We establish that, among different broadband polarization transfer schemes, the FLOPSY family[24] can be used to exchange magnetization between a *J* coupled

[†] Swiss Federal Institute of Technology.
[‡] Bruker AG.

(1) Grzesiek, S.; Anglister, J.; Ren, H.; Bax, A. *J. Am. Chem. Soc.* **1993**, *115*, 4369−4370.
(2) Browne, D. T.; Kenyon, G. L.; Packer, E. L.; Sternlic, H.; Wilson, D. M. *J. Am. Chem. Soc.* **1973**, *95*, 1316−1323.
(3) LeMaster, D. M. *Methods Enzymol.* **1989**, *177*, 23−43.
(4) LeMaster, D. M. *Annu. Rev. Biophys. Biophys. Chem.* **1990**, *19*, 243−266.
(5) LeMaster, D. M. *Q. Rev. Biophys.* **1990**, *23*, 133−174.
(6) Venters, R. A.; Farmer, B. T.; Fierke, C. A.; Spicer, L. D. *J. Mol. Biol.* **1996**, *264*, 1101−1116.
(7) Salzmann, M.; Pervushin, K.; Wider, G.; Senn, H.; Wuthrich, K. *J. Am. Chem. Soc.* **2000**, *122*, 7543−7548.
(8) Takahashi, H.; Nakanishi, T.; Kami, K.; Arata, Y.; Shimada, I. *Nat. Struct. Biol.* **2000**, *7*, 220−223.
(9) Tugarinov, V.; Muhandiram, R.; Ayed, A.; Kay, L. E. *J. Am. Chem. Soc.* **2002**, *124*, 10025−10035.
(10) Fernandez, C.; Adeishvili, K.; Wuthrich, K. *Proc. Natl. Acad. Sci. U.S.A.* **2001**, *98*, 2358−2363.
(11) Fernandez, C.; Hilty, C.; Bonjour, S.; Adeishvili, K.; Pervushin, K.; Wuthrich, K. *FEBS Lett.* **2001**, *504*, 173−178.
(12) Arora, A.; Tamm, L. K. *Curr. Opin. Struct. Biol.* **2001**, *11*, 540−547.
(13) Hwang, P. M.; Choy, W. Y.; Lo, E. L.; Chen, L.; Forman-Kay, J. D.; Raetz, C. R.; Prive, G. G.; Bishop, R. E.; Kay, L. E. *Proc. Natl. Acad. Sci. U.S.A.* **2002**, *99*, 13560−13565.
(14) Schubert, M.; Kolbe, M.; Kessler, B.; Oesterhelt, D.; Schmieder, P. *Chembiochem* **2002**, *3*, 1019−1023.
(15) Meier, S.; Haussinger, D.; Jensen, P.; Rogowski, M.; Grzesiek, S. *J. Am. Chem. Soc.* **2003**, *125*, 44−45.
(16) Wu, Z. R.; Bax, A. *J. Am. Chem. Soc.* **2002**, *124*, 9672−9673.
(17) Permi, P.; Rosevear, P. R.; Annila, A. *J. Biomol. NMR* **2000**, *17*, 43−54.
(18) Evenas, J.; Mittermaier, A.; Yang, D. W.; Kay, L. E. *J. Am. Chem. Soc.* **2001**, *123*, 2858−2864.
(19) Chou, J. J.; Bax, A. *J. Am. Chem. Soc.* **2001**, *123*, 3844−3845.
(20) Mittermaier, A.; Kay, L. E. *J. Am. Chem. Soc.* **2001**, *123*, 6892−6903.
(21) Oh, B. H.; Westler, W. M.; Darba, P.; Markley, J. L. *Science* **1988**, *240*, 908−911.
(22) Westler, W. M.; Kainosho, M.; Nagao, H.; Tomonaga, N.; Markley, J. L. *J. Am. Chem. Soc.* **1988**, *110*, 4093−4095.
(23) Eletsky, A.; Moreira, O.; Kovacs, H.; Pervushin, K. *J. Biomol. NMR* **2003**, *26*, 167−179.
(24) Kadkhodaie, M.; Rivas, O.; Tan, M.; Mohebbi, A.; Shaka, A. *J. Magn. Reson.* **1991**, *91*, 437−443.

10.1021/ja0381813 CCC: $27.50

network of spins while largely decoupling dipolar interactions between these spins. This property distinguishes FLOPSY from the WALTZ and MOCCA-SIAM rf-modulation schemes employed to exchange magnetization between dipolar coupled homonuclear spins.[25,26] Here, we demonstrate that (i) homonuclear dipolar decoupling during polarization transfer is important to eliminate the dependence of line-shape distortions in TOCSY spectra of *J* coupled spins[27,28] on the presence of dipolar interactions, which otherwise might result in biased $^{13}C-^{13}C$ RDC values, (ii) the homonuclear $^{13}C-^{13}C$ TOCSY provides an extensive set of side-chain $^{13}C-^{13}C$ RDCs which correlate well with the 3D structure, and (iii) the $^{13}C-^{13}C$ RDCs can be effectively cross-validated using more conventional backbone $^{1}H-^{15}N$ RDCs measured at a lower degree of molecular alignment.

Experimental Section

RDCs were determined using a 1.4 mM u-$^{2}H,^{13}C,^{15}N$ -labeled his_6-tagged human ubiquitin sample dissolved in 90%/10% H_2O/D_2O containing 10 mM potassium phosphate and 0.05% w/v sodium azide at pH 7.2. The sample with the aligned protein was obtained upon addition of Pf1 phages from a 50 mg/mL stock solution until the observed quadrupolar deuterium splitting of the $^{2}H_2O$ signal was 8 Hz. The [$^{15}N,^{1}H$]-correlation experiments were performed using a Bruker Avance 600 MHz spectrometer, equipped with a cryogenic Z-gradient TXI probe. The ^{13}C-start, ^{13}C-observe experiments were performed on a Bruker Avance 500 MHz spectrometer equipped with a cryogenic Z-gradient DUAL $^{13}C/^{1}H$ probe. All NMR experiments were performed at 20 °C. The 2D-[$^{13}C,^{13}C$]-TOCSY experiment was run as described by ref 23 except that FLOPSY-16 mixing was applied at $\gamma B_1 = 8.5$ kHz and with $\tau_{mix} = 16.96$ ms. The acquired 2D-[$^{13}C,^{13}C$]-TOCSY spectra of u-$^{2}H,^{13}C,^{15}N$-labeled ubiquitin are shown in Figure 1. The spectra were analyzed using the program XEasy.[29]

Theoretical Basis

$^{13}C-^{13}C$ and $^{1}H-^{15}N$ RDCs. For weak molecular alignment, the dipolar coupling between the spins *i* and *j*, D_{ij}, which depends on the axial component $A_a = (^3/_2)A_{zz}$ and the rhombicity $\eta = {}^2/_3(A_{xx} - A_{yy})/A_{zz}$ of the alignment tensor, where A_{xx}, A_{yy}, and A_{zz} are the Cartesian components in the principal axis system, is defined as described by:[30]

$$D_{ij} = S(\mu_0/4\pi)\gamma_i\gamma_j/r_{ij}{}^3(h/2\pi^2)A_a\{(3\cos^2\theta - 1)/2 + {}^3/_4\eta(\sin^2\theta\cos 2\phi)\} \quad (1.1)$$

where θ and ϕ describe the polar angles of the mean orientation of the $i-j$ interaction vector, S^2 is the generalized order parameter, μ_0 is the magnetic permeability of free space, γ_i is the gyromagnetic ratio of the spin *i*, *r* is the $i-j$ internuclear distance, and *h* is Planck's constant. Because on average the amplitude of D_{CC} is only $^1/_5$ of the D_{HN} values, it is instructive to measure $^{13}C-^{13}C$ and $^{1}H-^{15}N$ RDCs at higher and lower concentrations of the alignment media, respectively. In the irreducible tensor representation, the dipolar couplings are calculated as:[31]

$$D_{ij}^{clc} = \sum_{m=-2,2} A_m Y_{2m}(\theta_{ij},\phi_{ij}) \quad (1.2)$$

where Y_{2m} is the spherical harmonics, and A_m corresponds to the irreducible components of the Saupe order matrix[32] and is obtained by a linear fit of the measured RDCs values against calculated *D* values. Because the phages are fully aligned at both concentrations,[33,34] the Euler angles orienting the main axis system are expected to be the same, whereas the main components of the alignment tensor scale linearly with the Pf1 concentration. Under the assumption of a uniformly scaled S^2 for the C−C and H−N vectors, the independent measurements can be cross-validated: $^{13}C-^{13}C$ RDC values calculated from the scaled alignment tensor obtained from the $^{1}H-^{15}N$ measurements may be compared to the values calculated using the tensor obtained from the $^{13}C-^{13}C$ RDCs fit. In addition, the scalar

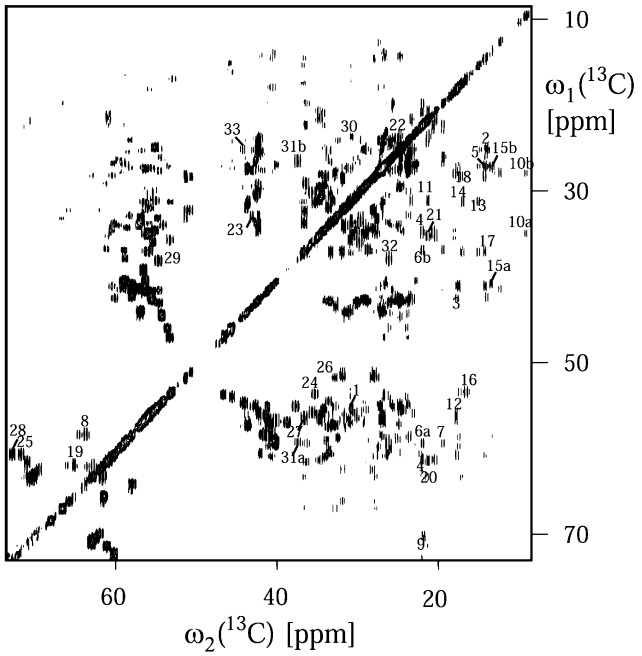

Figure 1. 2D-[$^{13}C,^{13}C$]-TOCSY spectrum measured with uniformly $^{2}H,^{13}C,^{15}N$-labeled ubiquitin ($T = 293$ K, 1.4 mM His-tagged human ubiquitin at pH 7.2 in 10 mM potassium phosphate buffer and 0.05% w/v sodium azide) recorded on a Bruker Avance spectrometer operating at a proton frequency of 500 MHz. The residual dipolar couplings were determined by comparing the splitting measured along the $^{13}C(\omega_2)$ dimension in a pair of the 2D-[$^{13}C,^{13}C$]-TOCSY spectra recorded on samples without and with addition of Pf1 phages (quadrupolar deuterium splitting of $^{2}H_2O = 8$ Hz). Selected cross-peaks whose multiplets were used in the analysis are marked with numbers, which correspond to the assignment listed in Tables 1 and 2. Letters count different cross-peaks which yield independently the same splitting values. In the experimental setup, the radio frequency carrier offsets were placed at 40 ppm (^{13}C), 173 ppm ($^{13}C'$), and 3.0 ppm (^{2}H). The 2D-[$^{13}C,^{13}C$]-TOCSY spectrum was recorded with $t_{1max} = 17.9$ ms and $t_{2max} = 203.2$ ms, an interscan delay of 2 s, and 180 × 4096 complex points resulting in an acquisition time of 20 h per spectrum. The mixing time was 16.96 ms. Before Fourier transformation, the time domain data in the t_1 and t_2 dimensions were multiplied by a cosine function and zero-filled to 1024 and 16 384 points, respectively.

(25) Moglich, A.; Wenzler, M.; Kramer, F.; Glaser, S. J.; Brunner, E. *J. Biomol. NMR* **2002**, *23*, 211−219.
(26) Hansen, M. R.; Rance, M.; Pardi, A. *J. Am. Chem. Soc.* **1998**, *120*, 11210−11211.
(27) Braunschweiler, L.; Ernst, R. R. *J. Magn. Reson.* **1983**, *53*, 521−528.
(28) Sorensen, O. W.; Rance, M.; Ernst, R. R. *J. Magn. Reson.* **1984**, *56*, 527−534.
(29) Bartels, C.; Xia, T. H.; Billeter, M.; Guntert, P.; Wuthrich, K. *J. Biomol. NMR* **1995**, *6*, 1−10.
(30) Tjandra, N.; Bax, A. *Science* **1997**, *278*, 1111−1114.
(31) Sass, J.; Cordier, F.; Hoffmann, A.; Cousin, A.; Omichinski, J. G.; Lowen, H.; Grzesiek, S. *J. Am. Chem. Soc.* **1999**, *121*, 2047−2055.
(32) Saupe, A. *Z. Naturforsch.* **1964**, *19A*, 161−171.
(33) Hansen, M. R.; Mueller, L.; Pardi, A. *Nat. Struct. Biol.* **1998**, *5*, 1065−1074.
(34) Clore, G. M.; Gronenborn, A. M. *Proc. Natl. Acad. Sci. U.S.A.* **1998**, *95*, 5891−8.

product between the normalized five-dimensional alignment vectors (A_{-2}, A_{-1}, A_0, A_1, A_2) can be used as a measure of the degree of collinearity.[31]

Line-Shape Distortions in TOCSY. In homonuclear 2D TOCSY spectra, line-shape distortions might arise due to the presence of the pulsed field gradient-insensitive zero-quantum coherence after the TOCSY mixing period along with the desired single spin polarization operators.[27,28] For a homonuclear dipolar and scalar coupled two-spin-$^1/_2$ system *IS*, the selected polarization transfer pathway under rf-irradiation resulting in the detectable signal is represented by eq 2.

$$I_z \rightarrow \mathrm{T}_{Iz\rightarrow Sz}(\tau)S_z + \mathrm{T}_{Iz\rightarrow ZQ}(\tau)ZQ \qquad (2)$$

where $ZQ \equiv -2(I_xS_y - I_yS_x)$, and the transfer functions $\mathrm{T}_{Iz\rightarrow Sz}(\tau)$ and $\mathrm{T}_{Iz\rightarrow ZQ}(\tau)$ are determined by spin−spin interaction Hamiltonians, chemical shifts of the involved spins, as well as the duration τ, strength, and modulation scheme of the rf-irradiation.[35]

A superposition of the residual dipolar coupling Hamiltonian, H_D, and the *J* coupling Hamiltonian, H_J, renders $\mathrm{T}_{Iz\rightarrow Sz}(\tau)$ and $\mathrm{T}_{Iz\rightarrow ZQ}(\tau)$ as functions of J_{IS} and D_{IS},[36] thus resulting in different distortions of the line shapes in the presence or absence of spatial molecular alignment and, consequently, introducing a bias to the measured values of RDCs. To analyze these functional dependencies, the analytical effective chemical shift nonperturbed Hamiltonian H^{eff} is calculated using the exact effective Hamiltonian theory (EEHT) introduced by Untidt and Nielsen.[37] We demonstrate both analytically and computationally (see Appendix) that the effective dipolar Hamiltonian is scaled down by a factor $s_D \approx -0.167$ when the FLOPSY pulse sequence is employed to exchange polarization between coupled ^{13}C spins. Thus, the problem of differential line shape in the presence and absence of dipolar Hamiltonians is essentially avoided.

Results and Discussion

The 2D ^{13}C−^{13}C correlation spectroscopy enables detection of all types of ^{13}C spin systems found in proteins excluding methyl ^{13}C spins of methionine. Depending on the number of ^{13}C spins directly attached to the directly observed ^{13}C spin and neglecting effects of long range $^{>1}J_{CC}$ couplings, ^{13}C,^{13}C-cross-peaks in the 2D-[^{13}C,^{13}C]-TOCSY spectrum are split in the ω_2 dimension into doublets, quadruplets (frequently with degenerate central components), and octets. ^{13}C−^{13}C RDCs can be effectively extracted from the doublet-split peaks stemming often from the structurally important methyl groups due to their good chemical shift dispersion and the splitting pattern. In addition, RDCs from quadruplet-split peaks stemming mostly from methylene groups can be measured. Figure 2 shows typical multiplet patterns extracted from 2D-[^{13}C,^{13}C]-TOCSY spectra. In the first step of our analysis, 23 ^{13}C−^{13}C RDCs were determined by subtracting the splitting observed in doublets of the aligned sample from those of the unaligned sample (Table 1). Only the cross-peaks which exhibited a sufficiently high signal-to-noise ratio and absence of spectral overlap were analyzed. The alignment tensor was obtained by optimizing the fit of the measured ^{13}C−^{13}C RDCs values against D_{CC} values calculated on the basis of the X-ray crystal structure of human ubiquitin[38] (PDB 1UBQ),[31] yielding a correlation coefficient of 0.988 and a root-mean-square deviation of 0.277 Hz (Figure 3a).

In the second step, the alignment tensor calculated using the ^{13}C doublets was employed to predict the splitting of the outer components of the ^{13}C quadruplets. The measurements of the

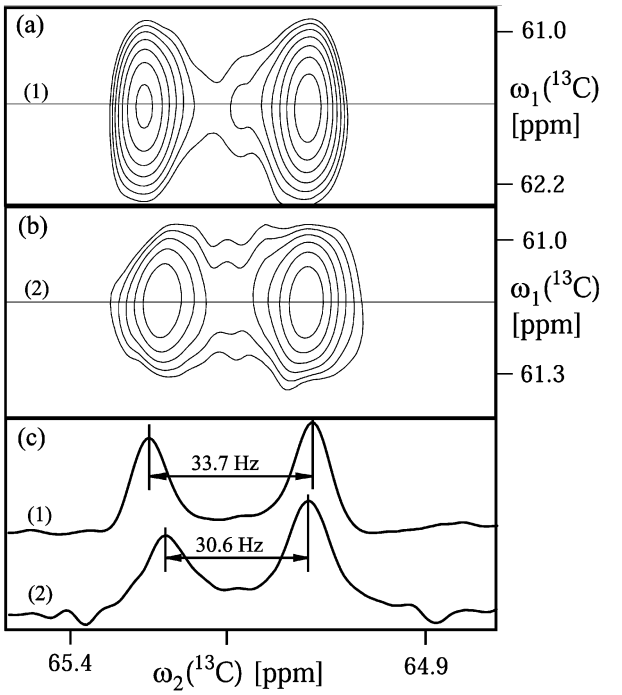

Figure 2. Expansions of the [$^{13}C^{\alpha}$,$^{13}C^{\beta}$] cross-peaks of Figure 1 (a) and upon addition of Pf1 (b). 1D cross-sections from the spectra of (a) and (b) are shown in (c). The measured distances between the doublet components of Ser65 are $^1J_{C\alpha C\beta} = 33.7$ Hz and $(^1J_{C\alpha C\beta} + D_{C\alpha C\beta}) = 30.0$ Hz, resulting in $D_{C\alpha C\beta} = -3.7$ Hz.

Table 1. Experimental and Theoretical D_{CC} Values Derived from ^{13}C Doublets

cross-peak[a]	residue	atom	D_{CC}^{exp}, [Hz]	D_{CC}^{clc}, [Hz]
1	Met1	C^{γ}	−0.9	−0.804
2	Ile3	$C^{\delta 1}$	−3.0	−2.885
3	Ile3	$C^{\gamma 2}$	−1.0	−1.418
4	Val5	$C^{\gamma 1}$	0.4	0.164
5	Ile13	$C^{\delta 1}$	−0.6	−0.789
6	Val17	$C^{\gamma 1}$	−1.1	−0.632
7	Val17	$C^{\gamma 2}$	2.6	2.752
8	Ser20	C^{β}	3.2	3.453
9	Thr22	$C^{\gamma 2}$	−0.1	−0.698
10	Ile23	$C^{\delta 1}$	−3.0	−3.155
11	Val26	$C^{\gamma 2}$	−1.1	−0.630
12	Ala28	C^{β}	1.1	1.001
13	Ile30	$C^{\delta 1}$	2.0	1.891
14	Ile30	$C^{\gamma 2}$	0.5	0.463
15	Ile36	$C^{\delta 1}$	1.0	1.175
16	Ala46	C^{β}	−0.6	−0.308
17	Ile61	$C^{\delta 1}$	0.9	0.433
18	Ile61	$C^{\gamma 2}$	−3.2	−2.950
19	Ser65	C^{β}	−3.7	−3.638
20	Thr66	$C^{\gamma 1}$	−0.7	−0.618
21	Val70	$C^{\gamma 1}$	1.1	0.887
22	Leu73	$C^{\delta 1}$	−0.5	−0.263
23	Arg74	C^{δ}	1.5	1.326

[a] Numbering of cross-peaks corresponds to the cross-peak annotation in Figure 1.

(35) Kramer, F.; Luy, B.; Glaser, S. J. *Appl. Magn. Reson.* **1999**, *17*, 173−187.
(36) Luy, B.; Glaser, S. J. *J. Magn. Reson.* **2001**, *148*, 169−181.
(37) Untidt, T. S.; Nielsen, N. C. *Phys. Rev. E* **2002**, *65*, art. no.-021108.
(38) Vijaykumar, S.; Bugg, C. E.; Cook, W. J. *J. Mol. Biol.* **1987**, *194*, 531−544.

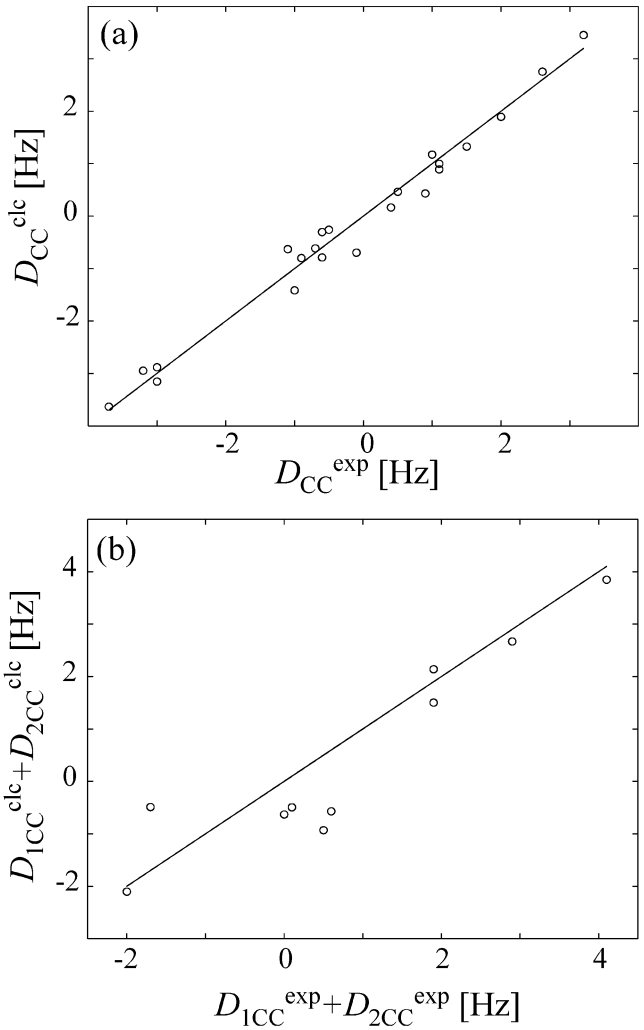

Figure 3. Calculated versus experimental values of D_{CC} of human ubiquitin measured using the 2D-[^{13}C,^{13}C]-TOCSY spectra. In (a) and (b), the correlations between calculated D_{CC}^{clc} and $D_{1CC}^{clc} + D_{2CC}^{clc}$ and experimental D_{CC}^{exp} and $D_{1CC}^{exp} + D_{2CC}^{exp}$ values are derived from the ^{13}C−$^{13}\underline{C}$ doublets and $^{13}C_1-^{13}\underline{C}-^{13}C_2$ quadruplets, respectively, where the $^{13}\underline{C}$ resonance is observed along the ω_2 dimension. The alignment tensor (see Table 3) was obtained by optimizing the fit between 23 D_{CC}^{exp} values obtained from ^{13}C doublets against D_{CC} values calculated on the basis of the X-ray crystal structure of human ubiquitin.[38] In (a), the correlation coefficient is 0.988. In (b), the alignment tensor obtained with the use of ^{13}C doublets was directly applied to calculate $D_{1CC}^{clc} + D_{2CC}^{clc}$, resulting in the correlation coefficient of 0.926.

outer components yield the sum of the RDC contributions of each of the two attached ^{13}C spins 1 and 2, $D_{1CC} + D_{2CC}$ (Table 2). Theoretically, the contribution from each individual RDC can be calculated starting from the outermost ^{13}C atom, which has a coupling to only one neighbor carbon. From here, each successive carbon splitting can be decomposed into the already known contribution of the carbon further out on the side chain and the unknown contribution of the neighbor closer to the backbone. The relatively small values of ^{13}C−^{13}C RDCs and large uncertainties in the RDC measurements render this technique impractical. Instead, the sum $D_{1CC} + D_{2CC}$ is used as a structural constraint.[39] A correlation coefficient of 0.926 and a root-mean-square deviation of 0.772 Hz between predicted and experimental sums $D_{1CC} + D_{2CC}$ are obtained for the 10 cross-peaks, showing no overlap and a sufficient signal-to-noise ratio (see Figure 3b). Because these RDCs were not used in the fitting of the alignment tensor, the good fit between theoretical and experimental $D_{1CC} + D_{2CC}$ values indicates that the tensor is correct. In all cases where a given RDC could be measured independently from different cross-peaks, the deviation between the measurements was less than 0.3 Hz, and the average was used. The sole exception was the splitting of $^{13}C^{\gamma}$ of Glu64 which can be measured independently from two peaks which show equal signal-to-noise ratios and are both well resolved, where the determined values are 0 and 1.9 Hz. In the case of 0 Hz, small peaks are observed between the multiplet components, which might perturb the apparent couplings. This fact favors the choice of 1.9 Hz which also is closer to the theoretical value of about 1.5 Hz.

Table 2. Experimental and Theoretical $D_{1CC} + D_{2CC}$ Values Derived from the ^{13}C Quadruplets

cross-peak[a]	residue	atom	$(D_{1CC} + D_{2CC})^{exp}$, [Hz]	$(D_{1CC} + D_{2CC})^{clc}$, [Hz]
24	Glu18	C^{γ}	0.6	−0.568
25	Thr22	C^{β}	−1.7	−0.488
26	Pro38	C^{β}	2.9	2.667
27	Glu51	C^{γ}	−2.0	−2.104
28	Thr55	C^{β}	1.9	2.143
29	Asn60	C^{α}	0.5	−0.930
30	Lys63	C^{γ}	0.1	−0.491
31	Glu64	C^{γ}	1.9	1.504
32	Glu64	C^{β}	0.0	−0.626
33	Leu67	C^{β}	4.1	3.844

[a] Numbering of cross-peaks corresponds to the cross-peak annotation in Figure 1.

The effects of the ^{13}C line-shape distortions due to the presence of the pulsed field gradient-insensitive zero-quantum coherencies after the TOCSY mixing period[27,28] on the ^{13}C−^{13}C RDCs measurements were analyzed by calculating the Taylor expansion of the exact effective Hamiltonian for a two-spin system coupled by scalar and dipolar interactions. The FLOPSY pulse sequence largely decouples dipolar coupled spins, attenuating the effective dipolar coupling constant by a factor of −0.167. Although the ^{13}C shapes in the ω_2 dimension can be significantly perturbed by a zero-quantum coherence converted to the detectable magnetization by the last ^{13}C 90° reading pulse, this perturbation is largely independent of the amplitude of RDCs, so that D_{CC} can still be reliably extracted as the difference between two measurements of the apparent maxima of the ^{13}C multiplets in the absence and presence of the alignment medium. For the parameters typically used for the ^{13}C−^{13}C TOCSY experiment, the residual, not suppressed part of the dipole/dipole coupling introduces a systematic bias to the measured values of D_{CC} at the level of 0.2%, which can be safely neglected.

The off-resonance propagation of the magnetization is analyzed by numerical calculations based on the H_D, H_J, and chemical shift Hamiltonians of the *IS* spin system in the rotating frame. Figure 4 shows the transfer functions $T_{Iz\rightarrow Sz}(\tau)$ and $T_{Iz\rightarrow ZQ}(\tau)$ calculated for τ = 16.96 ms with a variable offset frequency of spin *S* while spin *I* was kept synchronized with the rotating frame using D_{IS} = 20 Hz, J_{IS} = 35 Hz, and $\gamma_c B_1$ = 8.5 kHz. Although the off-resonance effects can increase the relative efficiency of the polarization transfer under H_D and H_J Hamiltonians, the systematic bias to the values of D_{CC} does not exceed a level of 1% throughout the polarization transfer bandwidth.

(39) Ottiger, M.; Delaglio, F.; Marquardt, J. L.; Tjandra, N.; Bax, A. *J. Magn. Reson.* **1998**, *134*, 365−369.

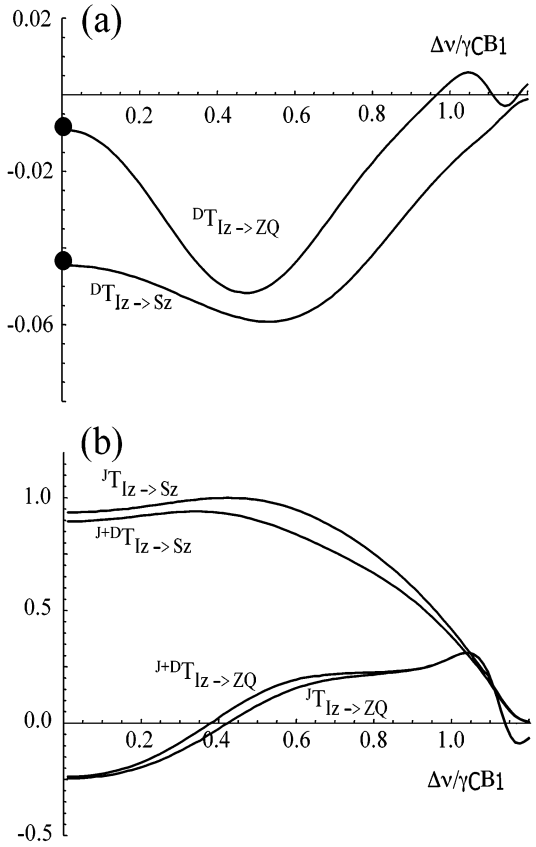

Figure 4. The polarization transfer functions $T_{Iz\rightarrow Sz}$ and $T_{Iz\rightarrow ZQ}$ calculated for the different offset frequencies of the spin *S* from the frequency of the spin *I* synchronized with the rotating frame. The evolution of the density operator I_{1z} via the [^{13}C,^{13}C]-TOCSY pulse sequence[23] with $t_1 = 0$ ms, $\tau_{mix} = 16.96$ ms, and $\gamma B_1 = 8.5$ kHz was calculated in the presence of the H_D (a) and $H_D + H_J$ (b) Hamiltonians. The filled circles in (a) represent values of the transfer functions $T_{Iz\rightarrow Sz}$ and $T_{Iz\rightarrow ZQ}$ calculated using the effective Hamiltonian of eqs 5 and 6 for the FLOPSY-2 mixing sequence of the total duration τ_{RR}*24 = 16.96 ms at $\gamma B_1 = 8.5$ kHz.

In general, for interacting spins *i* and *j* separated by the internuclear distance r_{ij}, D_{ij} is proportional to the product $\gamma_i\gamma_j/r_{ij}^3$. Therefore, one can predict that the maximal amplitude of D_{CC} in aliphatic side chains constitutes approximately $^1/_5$ of the amplitude of easily accessible backbone D_{HN} RDCs. Thus, to achieve optimal precision in both D_{CC} and D_{HN} measurements, it is reasonable to perform the latter at a somewhat lower concentration of alignment media. For example, backbone D_{HN} values in the range of ±20 Hz were achieved, which corresponds to an expected range of ±4 Hz for D_{CC} values. However, at these conditions, the signal-to-noise ratio in the [^{15}N,^{1}H]-correlation experiments was not sufficient for reliable alignment tensor calculations, so that the lower alignment degree was used to quantify D_{HN}. Therefore, a cross-validation of D_{HN} and D_{CC} required an appropriate scaling of the corresponding alignment tensors.

As an additional verification, we compared the alignment tensor to the corresponding alignment tensor derived from the independently measured backbone ^{1}H−^{15}N RDCs. Because of the severe line broadening observed in the [^{15}N,^{1}H]-correlation experiments, the lower Pf1 concentration was used. A comparison of the parameters of the tensors listed in Table 3 indicates a good correspondence between the two independently determined tensors. The Euler angles differ by less than 10°,

Table 3. Alignment Tensor Parameters

measured RDCs	$(3/2)A_{zz}S = A_aS$ [10^{-4}]	$A_{xx}S$ [10^{-4}]	$A_{yy}S$ [10^{-4}]	rhombicity	α [deg]	β [deg]	γ [deg]
^{13}C−^{13}C	10.72	−1.19	−9.53	0.519	147.7	56.0	45.9
^{1}H−^{15}N	5.96	−0.68	−5.29	0.515	139.0	48.0	49.0

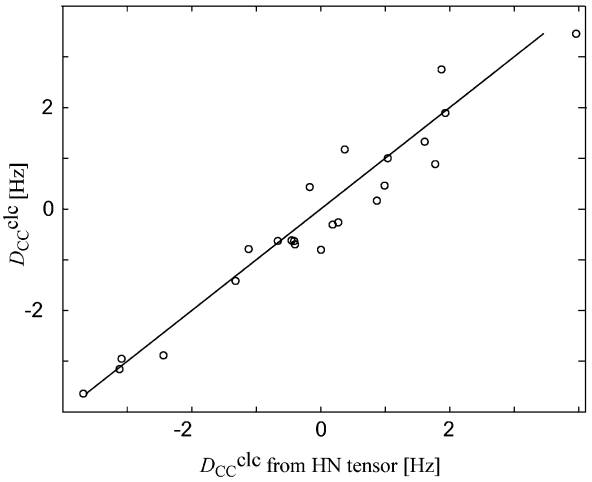

Figure 5. Calculated values of ^{13}C−^{13}C RDCs from the corresponding alignment tensor versus calculated values of ^{13}C−^{13}C RDCs using a scaled up alignment tensor obtained from the ^{1}H−^{15}N measurements. The correlation coefficient is 0.967, and the root-mean-square deviation is 0.484 Hz.

and the scaling factor is 0.56 ± 0.01 for all of the main components under the assumption of uniformly scaled order parameters S^2. The theoretical values of the ^{13}C−^{13}C RDCs were calculated using the scaled up alignment tensor obtained from the ^{1}H−^{15}N measurements. A comparison with theoretical values obtained from the original alignment tensor yields a correlation coefficient of 0.967 and a root-mean-square deviation of 0.484 Hz (Figure 5). The high degree of collinearity of these two tensors is also reflected in the 0.976 value for the scalar product between the normalized five-dimensional alignment vectors corresponding to the two alignment tensors.

Because we introduce a scaling factor to correlate ^{13}C−^{13}C RDCs obtained from a ^{13}C−^{13}C tensor with ^{13}C−^{13}C RDCs derived from a ^{1}H−^{15}N tensor, possible systematic differences between averaged order parameters S_{CC}^2 and S_{HN}^2 are absorbed into the scaling factor. Although we expect certain dynamical averaging of measured RDCs,[40,41] the high degree of correlation between two alignment tensors independently derived from ^{13}C−^{13}C RDCs and ^{1}H−^{15}N RDCs might indicate applicability of our simplified approach.

The effect of mobility of individual side chains can be evaluated using the generalized order parameters of C^γ spins independently derived from experimental $^3J_{NC\gamma}$ and $^3J_{C'C\gamma}$ (S_J^2), dipolar couplings (S_D^2),[41] and ^{2}H relaxation rates (S_{rel}^2).[42] For the long side chains of Ile3 ($C^{\gamma 2}$), Val5 ($C^{\gamma 1}$), Val17 ($C^{\gamma 1}$ and $C^{\gamma 2}$), Thr22 ($C^{\gamma 2}$), Val26 ($C^{\gamma 2}$), Ile30 ($C^{\gamma 2}$), Ile61 ($C^{\gamma 2}$), and Val70 ($C^{\gamma 1}$), for which all of these measurements are available, the averaged S^2 values usually do not deviate by more than 15%

(40) Tolman, J. R.; Al-Hashimi, H. M.; Kay, L. E.; Prestegard, J. H. *J. Am. Chem. Soc.* **2001**, *123*, 1416−1424.
(41) Chou, J. J.; Case, D. A.; Bax, A. *J. Am. Chem. Soc.* **2003**, *125*, 8959−8966.
(42) Lee, A. L.; Flynn, P. F.; Wand, A. J. *J. Am. Chem. Soc.* **1999**, *121*, 2891−2902.

from an overall average value of 0.81 except for Val26 (+20%) and Val70 (−58%). Although a significant discrepancy between S_J^2, S_D^2, and S_{rel}^2 is observed for some amino acids (e.g., for Ile3, these values cover a range from 0.38 (S_D^2) to 0.98 (S_{rel}^2)), the overall mobility of the core side chains is rather restricted. Note that in eq 1.1 S instead of S^2 is used. The averaged S values all stay within ±8% except for Val26 (+10%) and Val70 (−35%).

To simulate the effect of nonuniform S^2 values, all of the measured values in Table 1 were randomly changed within a range of ±20% (this corresponds to changes of S^2 values within ±40%). The main components of the alignment tensor change by less than 3%, and the Euler angles change by less than 1.5°. The calculated RDCs do not change more than 0.25 Hz, resulting in the correlation coefficient of 0.982. Thus, with the precision of our $^{13}C-^{13}C$ RDCs measurements around 15%, the use of uniform S^2 values for theoretical RDC calculations might be justified. It should be noted that, indeed, a weak correlation between $|D_{CC}^{exp}| - |D_{CC}^{clc}|$ and the average between S_J^2, S_D^2, and S_{rel}^2 was observed for all side chains with a sole exception of Val70, where the low-order parameter does not correlate with a good match between D_{CC}^{exp} and D_{CC}^{clc}. A possible source of this discrepancy might be a slightly shorter ubiquitin construct lacking residue 76 used in the current studies as compared to the construct used for the S^2 measurements and X-ray analysis, calling for a more detailed investigation. In a second simulation, we assumed that two arbitrarily selected side chains are highly mobile. The measured RDCs of the cross-peaks 3 and 13 in Table 1 were artificially reduced in input to calculations by 50%, corresponding to the reduction of S^2 by 75%. Even in this case, the orientation of the alignment tensor is only weakly affected (the Euler angles deviate by less than 3°), but the main components are downscaled by 22%, 7%, and 9%. Thus, calculated RDCs showed a variation within 0.5 Hz as compared to the unperturbed input, yielding a slightly lower correlation coefficient of 0.972. It can be concluded that, although the alignment tensor is determined rather correctly, the angular information pertinent to the specific bonds may be biased, so that care has to be taken when highly mobile side chains are analyzed.

The presently described approach to measure $^{13}C-^{13}C$ RDCs is limited, on one hand, by spectral overlap and, on the other hand, by the complex multiplet structure of many ^{13}C-correlation cross-peaks. This is usually observed for the ^{13}C spins covalently bound to ^{15}N or $^{13}C'$ spins. The availability of ^{13}C-detection cryo-probes and improvements in electronics enabling decoupling ^{15}N and $^{13}C'$ spins during signal acquisition shall significantly increase the number of cross-peaks amenable to extraction of useful RDCs. To alleviate spectral overlap, the use of spectrometers operating at higher magnetic field strength would be advantageous. A 2D-[^{13}C,^{13}C]-TOCSY spectrum recorded at the proton frequency of 900 MHz using a ^{13}C-detection, ^{2}H-,^{15}N-decoupling probe-head is available in the Supporting Information. Decoupling of ^{2}H, ^{15}N, and $^{13}C'$ during signal acquisition significantly simplifies the multiplet structure of cross-peaks. New experiments can be developed which utilize several magnetization transfer steps. We expect that the application of spin-state editing techniques such as homonuclear E.COSY will further simplify spectra and increase the number of side-chain RDCs obtained in highly deuterated proteins. The applicability of E.COSY to large proteins can be estimated on the basis of the line-width at half-peak height ($\Delta\nu_{1/2}$) of the $^{13}C^{aliphatic}$ spins of about 15 Hz observed in spectra of 44 kDa uniformly ^{2}H,^{13}C,^{15}N-labeled BsCM.[23] Assuming that useful spectral information can be extracted as long as the condition $\Delta\nu_{1/2} < {}^{1}J_{CC}$ is fulfilled, one would estimate that E.COSY experiments will be feasible up to 100 kDa proteins. Thus, direct detection of ^{13}C resonances in perdeuterated proteins for extracting a large number of side-chain $^{13}C-^{13}C$ RDC constraints shows promise as a new method of facilitating high-quality structure determination even for proteins larger than 40 kDa.

Acknowledgment. We thank Sebastian Meier and Dr. Florence Cordier for their help with the calculations and Dr. Fred Damberger for careful reading of this manuscript. Financial support was obtained from a Swiss National Science Foundation grant to K.V.P.

Appendix

Effective Hamiltonian for FLOPSY Mixing. The analytical expression is obtained for the effective chemical shift nonperturbed Hamiltonian H^{eff} using the exact effective Hamiltonian theory (EEHT).[37] Because H_D and H_J commute and H_J is invariant to coordinate frame transformations for on-resonance spins, only the dipolar effective Hamiltonian is considered. A minimal supercycle averaging out the chemical shift Hamiltonian is the FLOPSY-2 sequence, of the form $R\underline{R}$, where the element R is a symmetric composite pulse, and the underline indicates a phase shift of all constituent pulses by 180°.[24] The action of the sequence can be described by the product of 18 propagators, $U_{R\underline{R}} = U_{18} \ldots U_2U_1$, where

$$U_i = \exp[-i(\beta_i \cos \varphi_i(I_x + S_x) + \beta_i \sin \varphi_i(I_y + S_y) + 2\beta_i a_D \sqrt{6} T_{2,0})] \quad (3)$$

using the irreducible spherical tensor operator $T_{2,0} = (3I_zS_z - \boldsymbol{IS})/\sqrt{6}$, and where $a_D = \pi(2\pi D_{IS})/(2\omega_{rf})$ expresses the dependency on the angular frequencies for the dipolar coupling and the rf field amplitude $\omega_{rf} = 2\pi\gamma B_1$, and β_i is the rotational angle of the ith pulse applied with the phase φ_i. The homonuclear dipolar coupling Hamiltonian in the rotating frame using the high field approximation is defined as

$$H_D = 2\pi D_{IS} \sqrt{6} T_{2,0} \quad (4)$$

The individual propagators are transformed into the matrix representation followed by transformation of the concatenated propagator $U_{R\underline{R}}$ into the coupled basis. The coupled basis is commonly used to reduce the dimensionality of the problem and facilitate interpretations of the obtained operators in terms of spectral transitions. To avoid excessively complicated expressions, $U_{R\underline{R}}$ was expanded into a Taylor series around $a_D = 0$, and the expansion was truncated at the 10th order of a_D. Using the closed solution to the usual infinite series expansion of the logarithm of the $U_{R\underline{R}}$ propagator,[37] the effective Hamiltonian for the FLOPSY-2 sequence is obtained in the matrix form. The projection of the obtained effective Hamiltonian to the standard irreducible spherical tensor operators is given by eq 5, where for simplicity the Taylor expansion around

$a_D = 0$ is truncated at the 3rd order:

$$-iH^{\text{eff}}\tau_{\underline{\text{RR}}} = b_{2,1}T_{2,1} + (-b_{2,1})^*T_{2,-1} + b_{2,2}T_{2,2} + (-b_{2,2})^*T_{2,-2} + b_{2,0}\sqrt{6}T_{2,0} \quad (5)$$

and the symbol "*" denotes complex conjugation and $\tau_{\underline{\text{RR}}} = 23.55\tau_{90} = 23.55\pi/(2\omega_{\text{rf}})$, $-T_{2,\pm1} = \pm(I^{\pm}S_z + I_zS^{\pm})$ and $T_{2,\pm2} = {}^1/_2I^{\pm}S^{\pm}$.

$$b_{2,1} = (-0.05 + 2.50i)a_D + (3.99 + 0.37i)a_D{}^3 + O(a_D{}^5) \quad (6.1)$$

$$b_{2,2} = (-0.59 + 4.83i)a_D + (8.82 + 7.48i)a_D{}^3 + O(a_D{}^5) \quad (6.2)$$

$$b_{2,0} = -1.59ia_D - 1.26ia_D{}^3 + O(a_D{}^5) \quad (6.3)$$

Due to the reflection symmetry of the pulse sequence, all even-order terms of a_D vanish in $H^{\text{eff}}\tau_{\underline{\text{RR}}}$,[43] which is confirmed by an inspection of the Taylor expansion of eq 6 to higher orders.

Expressions similar to eqs 5 and 6 can also be derived using the zero-order average Hamiltonian theory formulated for the windowless cyclic pulse sequences.[44] Although not essential for the current application, the EEH theory has a clear advantage of providing a Taylor series of the exact effective Hamiltonian even in the case of a complicated pulse sequence, whereas the higher-order approximations of the effective Hamiltonian would be increasingly difficult to produce using the average Hamiltonian approach.

The form of the dipolar coupling Hamiltonian of eq 4 is not strictly conserved in the effective Hamiltonian of eqs 5 and 6, as is the case for the DIPSI-2, WALTZ, MLEV, and MOCCA pulse sequences. Nonetheless, it is instructive to find a new, tilted coordinate frame, where the term proportional to $\sqrt{6}T'_{2,0}$ has the largest amplitude. This frame is established by diagonalization of the normalized projection matrix $\langle H^{\text{eff}} | I_iS_j \rangle$ with $i, j = x, y$, and z[45] resulting in the effective Hamiltonian in the tilted frame with the z' axis tilted by 83.97°, 83.45°, and 8.92° from z, x, and y, respectively, and x' tilted by 148.48° from x:

$$H^{\text{eff}} = (-0.167)2\pi D_{IS}\sqrt{6}T'_{2,0} - (0.017)2\pi D_{IS}(2I_{x'}S_{x'} - 2I_{y'}S_{y'}) \quad (7)$$

Neglecting the second term in the Hamiltonian of eq 7, the dipolar scaling factor[45] $s_D \approx -0.167$ is obtained, which can be compared to the s_D values of -0.5, 1, and 0.25 calculated for the DIPSI-2, MOCCA-XY16, and MLEV-16 schemes.

Supporting Information Available: Figure showing a ^{2}H-, ^{15}N-, and ^{13}C′-decoupled 2D-[^{13}C,^{13}C]-TOCSY spectrum recorded on a Bruker Avance spectrometer operating at the proton frequency of 900 MHz (PDF). This material is available free of charge via the Internet at http://pubs.acs.org.

JA0381813

(43) Mansfiel, P.; Orchard, M. J.; Stalker, D. C.; Richards, K. H. *Phys. Rev. B* **1973**, *7*, 90−105.
(44) Burum, D. P.; Linder, M.; Ernst, R. R. *J. Magn. Reson.* **1981**, *44*, 173−188.
(45) Kramer, F.; Glaser, S. J. *J. Magn. Reson.* **2002**, *155*, 83−91.